

# How good are my data? Reference standards in superresolution microscopy

Markus Mund<sup>a</sup> and Jonas Ries<sup>b,\*</sup>

<sup>a</sup>Department of Biochemistry, University of Geneva, 1211 Genève, Switzerland; <sup>b</sup>European Molecular Biology Laboratory, Cell Biology and Biophysics, 69117 Heidelberg, Germany

**ABSTRACT** Superresolution microscopy is becoming increasingly widespread in biological labs. While it holds enormous potential for biological discovery, it is a complex imaging technique that requires thorough optimization of various experimental parameters to yield data of the highest quality. Unfortunately, it remains challenging even for seasoned users to judge from the acquired images alone whether their superresolution microscopy pipeline is performing at its optimum, or if the image quality could be improved. Here, we describe how superresolution microscopists can objectively characterize their imaging pipeline using suitable reference standards, which are stereotypic so that the same structure can be imaged everywhere, every time, on every microscope. Quantitative analysis of reference standard images helps characterizing the performance of one's own microscopes over time, allows objective benchmarking of newly developed microscopy and labeling techniques, and finally increases comparability of superresolution microscopy data between labs.

## Monitoring Editor

David G. Drubin  
University of California,  
Berkeley

Received: Oct 29, 2019

Revised: Jun 16, 2020

Accepted: Jul 5, 2020

## BACKGROUND

Fluorescence microscopy has become a bread-and-butter tool in cell biology, with an ever-increasing variety of imaging techniques offering a suitable microscope for almost every biological question. Recently, this repertoire has been extended by so-called superresolution microscopy techniques, which pushed the obtainable resolution down to a few tens of nanometers or even below (Hell and Wichmann, 1994; Betzig *et al.*, 2006; Rust *et al.*, 2006). This is the size range of many cellular structures, including organelles and macromolecular machineries, and consequently superresolution microscopes quickly went to the top of the wish lists of many researchers. However for a few years, biological discoveries using superresolution microscopes remained scarcer than anticipated. This lag phase was largely because superresolution microscopy is a complex imaging modality unforgiving to imperfect image acquisition, sample quality, and computational analyses.

Nowadays superresolution microscopy, most prominently SMLM (single-molecule localization microscopy, which includes PALM/STORM [Betzig *et al.*, 2006; Rust *et al.*, 2006] and DNA-PAINT [Jungmann *et al.*, 2014]) and STED (stimulated emission depletion microscopy [Hell and Wichmann, 1994]), have become impactful tools in many biological labs. Nevertheless, even today, these methods remain complex to use, and often “secrets” and “special tricks” from experienced microscopists are needed in order to get great superresolution images (Jimenez *et al.*, 2019; Schermelleh *et al.*, 2019). Consequently, the literature contains superresolution images of widely varying quality, possibly because superresolution imaging critically depends on numerous parameters including microscope optics, fluorophores, sample quality, and a series of image processing steps, all of which need to be optimized. Thus, it can be hard for the reader of a paper—who is only able to look at the rendered superresolution images—to know how good these images are and to relate the conclusions presented in that paper to the underlying superresolution data.

DOI:10.1091/mbc.E19-04-0189

\*Address correspondence to: Jonas Ries (jonas.ries@embl.de).

Abbreviations used: FRC, Fourier ring correlation; NPC, nuclear pore complex; PSF, point spread function; SMLM, single-molecule localization microscopy.

© 2020 Mund and Ries. This article is distributed by The American Society for Cell Biology under license from the author(s). Two months after publication it is available to the public under an Attribution–Noncommercial–Share Alike 3.0 Unported Creative Commons License (<http://creativecommons.org/licenses/by-nc-sa/3.0>).

“ASCB®,” “The American Society for Cell Biology®,” and “Molecular Biology of the Cell®” are registered trademarks of The American Society for Cell Biology.

## RESOLUTION IN SUPERRESOLUTION MICROSCOPY

It is not trivial to quantify and report the resolution of superresolution microscopy images, because estimating the resolution by finding the closest features that still appear separate can be very inaccurate when the underlying structure is unknown. This is why, in SMLM, the localization precision is often reported, which must not be confused with resolution. The localization precision describes how precisely the positions of *individual* molecules have been

determined and is defined as SD of localizations around the true position of the fluorophore (Thompson *et al.*, 2002). It can be experimentally measured from the scattered cluster of localizations from a single fluorophore (for this, a single antibody is often identified in the image) (Huang *et al.*, 2008). In most cases, however, the reported localization precision is calculated directly in the fitting software and thus represents a theoretical best-case estimate. This can easily be wrong if incorrect parameters are used during the fitting, if the fitting is bad, or if sample drift and other instabilities occur during the imaging.

Besides the localization precision, the real image resolution crucially depends on the labeling efficiency. As a rule of thumb, for a continuous structure, any given resolution requires at least twice as high a labeling density (Legant *et al.*, 2016). Because current fluorophores and imaging modalities routinely yield localization precisions well below 10 nm, which approaches the size of individual proteins, it is often the labeling density that limits the resolution and not the localization precision.

So, can the resolution be calculated from a superresolution image, where the labeling density is usually unknown? Fourier ring correlation (FRC; Nieuwenhuizen *et al.*, 2013), a common approach to quantify resolution in electron microscopy, calculates a resolution metric directly from the localization data. It is, however, limited in distinguishing real structures from apparent structures caused by individual fluorophores. Because individual fluorophores blink multiple times, they cause clusters of localizations that have a high self-correlation and thus a higher FRC resolution.

Another approach to estimate imaging quality relies on comparing conventional (diffraction-limited) and superresolution images of the same field of view (Culley *et al.*, 2018), which informs about artifacts related to the actual superresolution imaging, but only detects artifacts that are so big that they would be visible in diffraction-limited images.

## REFERENCE STANDARDS ARE AN OBJECTIVE INDICATOR OF IMAGE QUALITY

So unfortunately, there is no “push-button” software to quantitatively analyze the quality of superresolution images. However, with standardized reference samples, which should give identical images every time, it is possible to measure directly how well the entire imaging pipeline is performing, including sample preparation, labeling, imaging, and data fitting. This principle is similar to many widely used methods in cell biology where quality control experiments, such as including loading controls in Western blots, are always performed and even shown alongside the actual data to give a direct indication of data quality.

Generally, such standard samples should have a defined structure where the fluorescent labels are precisely positioned with distances to each other that can be resolved by superresolution microscopy; they should be usable with common labels and tagging schemes, they should be present in large numbers per field of view to get meaningful statistics, and they should be accessible and easy to prepare.

In the following, we introduce suitable reference standards and discuss how they can be used to assess SMLM images (Supplemental Table S1 contains an overview of common reference standards). We then present a general strategy that allows any user to judge their SMLM experiments objectively for themselves.

## CHECK THE POINT SPREAD FUNCTION (PSF) WITH BEADS

First, it is essential to check if the microscope is optically aligned properly. For this, the PSF of the microscope is measured by

recording a z-stack of fluorescent beads. If the fluorescent spots in the raw images are bigger than the theoretical size calculated from the diffraction limit, this indicates imperfect optical alignment of the microscope that decreases the achievable signal-to-noise and resolution. Moreover, inspecting the PSF images over the z-range readily reveals common optical aberrations (Figure 1A). If strong, these aberrations will decrease localization precision and accuracy, induce image distortions, and can warrant realignment of the microscope.

For 3D imaging, the PSF images are then used to calculate a calibration curve or an experimental PSF model, which can account for PSF aberrations (Li *et al.*, 2018). For multi-color imaging, the PSFs of the different channels should be evaluated for chromatic shifts. As an alternative to using fluorescent beads, microscope calibration slides can be used to calibrate the PSF and chromatic aberration.

## CHECK THE MICROSCOPY PIPELINE WITH REFERENCE STANDARDS

Next, several images are acquired from reference standards under conditions as similar as possible to the final experiment. For this, ideally the reference structure is labeled with the same labeling strategy, dyes, and buffers as in subsequent experiments. These images are then used to benchmark various parameters, as detailed below.

The most frequently used standard sample has traditionally been microtubules immunolabeled in cells (Heilemann *et al.*, 2008; Huang *et al.*, 2008; Dempsey *et al.*, 2011), which readily give good images due to their clear filament structure (Figure 1B), but are limited in their quantitative interpretation, as discussed later. In addition, various other standards are used in the field. Most notably, DNA-based nanostructures represent a very versatile class of standards (Steinhauer *et al.*, 2009; Iinuma *et al.*, 2014; Zanicchi *et al.*, 2017) (Figure 1C). In these, the fluorophores can be designed to be precisely positioned in 3D, which is ideal in creating resolution standards. On the downside, these structures are somewhat limited in their choice of label (i.e., they are usually labeled with organic dyes and not photoswitchable fluorescent proteins) and are outside the cell, making them fundamentally different from the intracellular structures that are imaged in the actual experiment.

Generally, naturally occurring intracellular structures with precisely defined geometries are ideally suited as the reference standard. For instance, our lab recently harnessed the nuclear pore complex (NPC) as such a standard (Figure 1D; Thevathasan, Kahnwald, *et al.*, 2019), which we will use here as an example to explain how to determine three key parameters that determine the quality of superresolution images.

### Measure image resolution

The resolution can be directly measured from reference standard images. Because the distances between fluorophores in reference standards are known, they serve as molecular rulers that reveal which resolution is achieved in the image.

A classical approach has been to evaluate line profiles of microtubules, where the width of the line profiles was used as proxy for resolution. This is problematic, as underlabeled microtubules as well as measurements with a high fraction of overlapping blinking events also give narrower profiles, although they actually lead to a lower resolution. Second, the double peaks with a distance of about 25 nm (35 nm including primary and secondary antibodies to label microtubules; Dempsey *et al.*, 2011), which result from the 2D projection of a hollow cylinder, can only be used to confirm that a resolution of at least 25 nm (or 35 nm) was reached. We do not recommend this approach, because often only an individual or a few

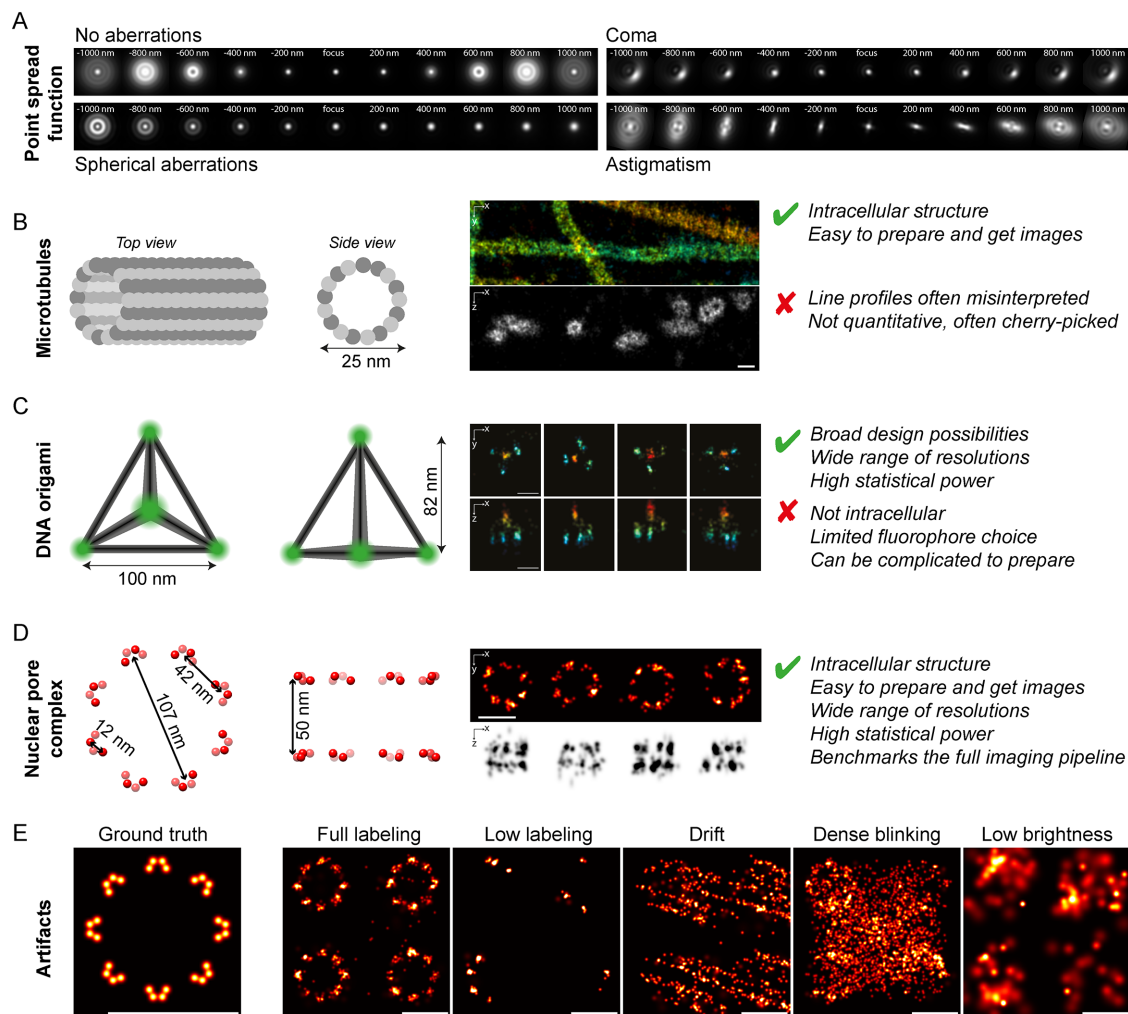


**FIGURE 1:** (A) PSF characterization using fluorescent beads. Simulated series of z-slices through PSFs with different aberrations. Spherical aberrations arise from refractive index mismatch between immersion medium and the specimen and can be compensated by using the correction collar of the objective, or refractive index matching. Coma and astigmatic aberrations indicate optical misalignment or suboptimal optical components in the microscope. (B–D) Commonly used reference standards for superresolution microscopy. (B) Microtubules were immunolabeled using primary/secondary antibodies and imaged using DNA-PAINT with an Atto655–conjugated imager strand (adapted with permission from Li *et al.*, 2018). (C) The corners of DNA origami tetrahedra were imaged using DNA-PAINT with an Atto655–conjugated imager strand (adapted with permission from Deschamps *et al.*, 2014), and (D) NPC protein Nup96–GFP stained with an Alexa Fluor 647–conjugated anti-GFP–nanobody (x–y views) or tagged with SNAPtag–Alexa Fluor 647 (x–z views) and imaged using STORM (adapted with permission from Thevathasan, Kahnwald, *et al.*, 2019). (E) Common artifacts in superresolution microscopy. Simulated SMLM images of NPC protein Nup96 highlight the common factors that deteriorate image quality. Scale bars 100 nm.

sections of a few microtubules are evaluated, and it is therefore prone to cherry picking and usually not quantitative.

Favorably, the NPC (Figure 1D) directly reveals if the resolution surpasses 107 nm (ring diameter), 42 nm (distance between corners), or 12 nm (distance of proteins within individual corners) in x–y and 50 nm in 3D (distance between the two rings; Thevathasan, Kahnwald, *et al.*, 2019). Hundreds of NPCs per individual image readily offer high statistical power. In addition to measuring image resolution, comparing the measured distances to these known values allows validating the spatial microscope calibration as well.

### Detect common artifacts

In general, a lot can be learned from “just looking at the thing.” This includes a few of the most common sources for suboptimal image

quality (see simulated images in Figure 1E): If the image shows a (directional) blur, this hints toward sample drift or stage vibration. If structures appear broken, fixation (which is almost always used in superresolution imaging) might have failed. If the reference structures appear incomplete, or are not resolved at all, the labeling or choice of fluorophore was suboptimal. If localizations are smeared out and appear in between the structures, the density of blinking events was too high, leading to spurious localizations in between the true positions of the emitters. Besides qualitative observation if the expected structural features are visible, a statistical analysis of the photoblinking reveals if photon counts, background, and calculated localization precision are within the expected range, indicating whether experimental parameters such as laser irradiance or buffer conditions were correct.

## Determine the effective labeling efficiency

As discussed earlier, a crucial determinant for the resolution in superresolution images is the labeling density, that is, how densely the structure of interest is decorated with detectable fluorophores (Legant *et al.*, 2016). The NPC standards allow a straightforward quantification of effective labeling efficiencies by counting the number of corners in hundreds of NPCs and fitting the distribution of corner numbers with a simple stochastic model (Thevathasan, Kahnwald, *et al.*, 2019). Measuring effective labeling efficiencies is crucial because they vary substantially between different labels and tags. For a variety of widely used labeling schemes, effective labeling efficiencies can range from more than 70% to as low as 20% (Thevathasan, Kahnwald, *et al.*, 2019), with obvious dramatic consequences for the achievable resolution. Furthermore, labeling reagents can deteriorate over time, which leads to suboptimal image quality and can be avoided by regular reference sample measurements.

Finally, reference standards guide the way to systematically optimizing the experiment: An insufficient labeling efficiency recommends new reagents or a different labeling scheme, a poor resolution on an otherwise well-labeled sample points to bad optical performance or image acquisition parameters, and so on.

## Analysis software

Besides sample preparation and imaging, optimal data processing is essential, as SMLM does not directly produce a superresolution image. The raw movies are fitted to obtain a list of localizations, which is typically postprocessed to filter out imprecise localizations and to correct for sample drift, before a superresolution image is reconstructed. The highly computational image generation makes it essential for the user to fully control the involved steps. Especially when superresolution images are analyzed quantitatively, it is crucial to test how parameter choices affect the analyses in order to ensure that the resulting data and their biological interpretation are robust.

This full control can be impossible to achieve with software packages that are bundled with commercial microscopes, which tend to perform processing steps as black boxes to simplify their use. Thus, we recommend choosing from the variety of SMLM software developed by the community (Supplemental Table S2), many of which are open source and have been thoroughly benchmarked. Just as for sample preparation and imaging, reference standard samples help SMLM users to ensure that the software is set up correctly, and the image analysis pipeline is performing optimally.

## CONCLUSIONS

Images and statistics from reference standard measurements provide an objective, realistic way to benchmark the performance of any microscopy pipeline. Also, they can be used to robustly test new developments in superresolution microscopy, which we envision will continue to have a growing impact in biological research. We hope that reference standards can allow the field to adopt common practices and increase transparency and comparability of superresolution imaging between labs. Examples of other techniques like x-ray crystallography and electron microscopy show how much can be gained from standardized image quality control—both for users and for other researchers, who are interpreting the data of their colleagues.

## ACKNOWLEDGMENTS

We thank Yiming Li for help with the PSF simulations. M.M. acknowledges support by an EMBO Long-Term Fellowship; J.R. acknowledges support by the European Research Council (grant no. ERC CoG-724489).

## REFERENCES

Boldface names denote co-first authors.

- Betzig E, Patterson GH, Sougrat R, Lindwasser OW, Olenych S, Bonifacio JS, Davidson MW, Lippincott-Schwartz J, Hess HF (2006). Imaging intracellular fluorescent proteins at nanometer resolution. *Science* 313, 1642–1645.
- Culley S, Albrecht D, Jacobs C, Pereira PM, Leterrier C, Mercer J, Henriques R (2018). Quantitative mapping and minimization of super-resolution optical imaging artifacts. *Nat Methods* 15, 263–266.
- Dempsey GT, Vaughan JC, Chen KH, Bates M, Zhuang X (2011). Evaluation of fluorophores for optimal performance in localization-based super-resolution imaging. *Nat Methods* 8, 1027–1036.
- Deschamps J, Mund M, Ries J (2014). 3D superresolution microscopy by supercritical angle detection. *Opt Express* 22, 29081–29091.
- Heilemann M, van de Linde S, Schüttelz M, Kasper R, Seefeldt B, Mukherjee A, Tinnefeld P, Sauer M (2008). Subdiffraction-resolution fluorescence imaging with conventional fluorescent probes. *Angew Chem Int Ed* 47, 6172–6176.
- Hell SW, Wichmann J (1994). Breaking the diffraction resolution limit by stimulated emission: stimulated-emission-depletion fluorescence microscopy. *Opt Lett* 19, 780–782.
- Huang B, Wang W, Bates M, Zhuang X (2008). Three-dimensional super-resolution imaging by stochastic optical reconstruction microscopy. *Science* 319, 810–813.
- Iinuma R, Ke Y, Jungmann R, Schlichthaerle T, Woehrstein JB, Yin P (2014). Polyhedra self-assembled from DNA tripods and characterized with 3D DNA-PAINT. *Science* 344, 65–69.
- Jimenez A, Friedl K, Leterrier C (2019). About samples, giving examples: optimized procedures for single molecule localization microscopy. *Methods* 174, 100–114.
- Jungmann R, Avendaño MS, Woehrstein JB, Dai M, Shih WM, Yin P (2014). Multiplexed 3D cellular super-resolution imaging with DNA-PAINT and Exchange-PAINT. *Nat Methods* 11, 313–318.
- Legant WR, Shao L, Grimm JB, Brown TA, Milkie DE, Avants BB, Lavis LD, Betzig E (2016). High-density three-dimensional localization microscopy across large volumes. *Nat Methods* 13, 359–365.
- Li Y, Mund M, Hoess P, Deschamps J, Matti U, Nijmeijer B, Sabinina VJ, Ellenberg J, Schoen I, Ries J (2018). Real-time 3D single-molecule localization using experimental point spread functions. *Nat Methods* 15, 367–369.
- Nieuwenhuizen RPJ, Lidke KA, Bates M, Puig DL, Grünwald D, Stallinga S, Rieger B (2013). Measuring image resolution in optical nanoscopy. *Nat Methods* 10, 557–562.
- Rust MJ, Bates M, Zhuang X (2006). Sub-diffraction-limit imaging by stochastic optical reconstruction microscopy (STORM). *Nat Methods* 3, 793–796.
- Schermelleh L, Ferrand A, Huser T, Eggeling C, Sauer M, Biehlmaier O, Drummen GPC (2019). Super-resolution microscopy demystified. *Nat Cell Biol* 21, 72–84.
- Steinhauer C, Jungmann R, Sobey TL, Simmel FC, Tinnefeld P (2009). DNA origami as a nanoscopic ruler for super-resolution microscopy. *Angew Chem Int Ed* 48, 8870–8873.
- Thevathasan JV, Kahnwald M, Cieślirski K, Hoess P, Peneti SK, Reitberger M, Heid D, Kasuba KC, Hoerner SJ, Li Y, *et al.*** (2019). Nuclear pores as versatile reference standards for quantitative superresolution microscopy. *Nat Methods* 16, 1045–1053.
- Thompson RE, Larson DR, Webb WW (2002). Precise nanometer localization analysis for individual fluorescent probes. *Biophys J* 82, 2775–2783.
- Zanacchi FC, Manzo C, Alvarez AS, Derr ND, Garcia-Parajo MF, Lakadamyali M (2017). A DNA origami platform for quantifying protein copy number in super-resolution. *Nat Methods* 14, 789–792.